

PROBING THE GALACTIC HALO ALONG THE 3C 273 SIGHT LINE USING *IUE*

GEOFFREY S. BURKS AND DONALD G. YORK¹

Astronomy and Astrophysics Center, The University of Chicago, 5640 Ellis Avenue, Chicago, IL 60637

J. CHRIS BLADES AND RALPH C. BOHLIN

Space Telescope Science Institute, 3700 San Martin Drive, Baltimore, MD 21218

AND

WILLEM WAMSTEKER

ESA, Apartado: 54065, 28080 Madrid, Spain

Received 1991 February 21; accepted 1991 April 12

ABSTRACT

High-resolution spectra of the QSO 3C 273 were obtained in 1989 and added to two spectra recorded in 1982. The co-added spectra represent 600,000 s of integration at a resolution of 30 km s^{-1} from 1200 to 2000 Å. The line of sight passes through the Virgo Cluster the entire halo of the Milky Way, at Galactic latitude $b = 64^\circ$, and foreground X-ray-emitting material from local disturbed gas. The observed equivalent width of Galactic C IV is greater than the equivalent width of C II, a situation that is uncommon in local gas but is often found in QSO absorption line systems. The lines of C IV, Al III, and Si IV may arise in an extended halo or may be associated with local disturbed gas in a radio loop. The remaining detected species (H I, C II, Si II) arise predominately from the local gas. Most of the gas is probably within 5 kpc, but no firm conclusion is reached. Possible detection of interstellar absorption due to the Virgo Cluster is discussed.

Subject headings: galaxies: clustering — interstellar: matter — quasars — ultraviolet: spectra

1. INTRODUCTION

The makeup of the Galactic halo has been studied and debated for years. The *IUE* (*International Ultraviolet Explorer*) satellite has offered the first possibility to study elements and ionization stages unavailable to ground-based observers. One of the problems is to know how the halo changes with height above the Galactic disk (Savage & de Boer 1981; Savage 1987). Evidence that this halo exists comes from the work of Reynolds (1990) on Galactic diffuse H α emission, from studies of optical absorption in high-latitude stars, and from radio measurements of Faraday rotation, interstellar scintillation, and pulsar dispersion measures (Spitzer 1978, chap. 3). All of these techniques argue for an ionized halo with an extent small compared with the Galactic diameter (York 1982a). By contrast, the halo might extend to a few Galactic radii, if it is as large as the halos postulated to explain the numerous absorption systems in spectra of quasi-stellar objects (Bahcall & Spitzer 1969).

A spectrum of the QSO 3C 273 gives a view through the entire halo and is also behind the Virgo Cluster. The QSO 3C 273 is one of the brightest quasi-stellar objects ($m_v = 12.9$). At a high latitude ($l = 289^\circ 95'$, $b = 64^\circ 38'$), the QSO can serve as a probe for hot gas in the halo. Ulrich et al. (1980) reported low-resolution absorption in the spectrum of 3C 273 and discussed the existence of a highly ionized halo. Strong ($> 200 \text{ mÅ}$) lines of C IV and Si IV attributable to gas in our Galaxy are seen in spectra of Magellanic Cloud stars and of Galactic stars with $|z| > 1 \text{ kpc}$ (Pettini & West 1982; Savage & de Boer 1981). Stars at distances of less than 1 kpc do not usually have absorption lines of C IV with equivalent widths in excess of 50 mÅ (Cowie, Taylor, & York 1981b).

Others have done high-resolution work on 3C 273 in the visual part of the spectrum by studying the Na I and Ca II lines

(Blades & Morton 1983; Cowie, Songaila, & York 1981a; Songaila & York 1980). York et al. (1983) studied Si IV halo absorption in 3C 273. In this paper, the spectra of more species are extracted and studied. The equivalent widths are presented and discussed, as is possible absorption by the Virgo Cluster.

2. *IUE* DATA

The data presented in this paper are the result of extracting and co-adding 10 *IUE* spectra obtained with the SWP camera (1200–2000 Å) in the high-resolution mode. These images were taken on double or triple observing shifts, sometimes exposing continuously for more than 16 hr, and are listed in Table 1. Data reduction was done in-house working from the *IUE* photometrically corrected image (PI) files. Spectra were extracted from the PI images and converted to intensity versus pixel plots. Extractions of the orders studied were done in the following manner. Images were rotated to rectify the spectra along lines of the SEC vidicon tube. Backgrounds were computed by averaging, then smoothing, lines on either side of the order. Lines (or rows of pixels) with appreciable signal (usually five) were summed and the background subtracted to get an extracted spectrum. This method gives better control over possible sources of error (York et al. 1982). These extractions were shifted in pixel space until they had a common wavelength solution and then added so as to improve the signal-to-noise ratio. The wavelength scale was derived from the standard *IUE* extractions and transferred to our own extractions using obvious spectral artifacts such as fiducial marks. Extractions for this paper were done in the same manner as is described in Burks et al. (1992) for RR Lyr stars and York et al. (1982) for AGNs.

Extracted data are shown in Figure 1. The spectra are shown in velocity space for the species listed. The range is from ~ 500 to 2000 km s^{-1} . The velocities shown are heliocentric; to convert to LSR, add 2.3 km s^{-1} (York et al. 1983). The spectra

¹ Also Enrico Fermi Institute, The University of Chicago.

TABLE 1
IMAGE LOG

Image	Day	Year	Exposure Time (minutes)
SWP 16786.....	108	1982	765
SWP 16791.....	109	1982	825
SWP 35466.....	31	1989	845
SWP 35469.....	33	1989	1080
SWP 35472.....	34	1989	825
SWP 36561.....	172	1989	1015
SWP 36563.....	173	1989	920
SWP 36572.....	175	1989	930
SWP 36574.....	176	1989	961
SWP 36576.....	177	1989	918

are shown in relative intensity units. Each spectrum is offset one unit above the previous (lower) spectrum. Zero points for the 10 spectra are numbered from 1 to 10. Reseau marks are shown by the letter R. "E" denotes the average velocity of the Virgo Cluster elliptical galaxies, and "B" and "C" denote the average velocities of the B and C subgroups of the Virgo Cluster spiral galaxies (de Vaucouleurs 1982). "G" denotes each of the positions of the H I geocorona line from *IUE* (from two apertures). The lines presented are, from top to bottom, Si IV 1402.770, Si IV 1393.755, Si II 1526.7066, Al III 1854.7164, Al III 1862.7895, Fe II 1608.4511, C IV 1548.195, C IV 1550.770, C II 1334.5323, and H I 1215.6737. Wavelengths are from Morton (1991). In the spectrum of H I (*bottom spectrum*), the strong geocoronal emission line has been suppressed. It would peak at 30 on this graph. One geocoronal line (first "G" from the left) is due to light through the large *IUE* aperture. The second line is due to flux through the small aperture (which peaks at 8). The roll-off in each plot at the edges is caused by the blaze function of the echelle grating. These spectra are not flattened or normalized.

York et al. (1983) reduced only Si IV in four spectra available at that time because the two resonance lines lie near the peak of the redshifted Lyman-alpha emission of 3C 273. All other parts of the spectrum have lower flux levels. Table 2 shows the flux in the wavelength regions of other lines from a low-resolution *IUE* spectrum of 3C 273 (York et al. 1983; Kinney et al. 1991). More data are needed to find sufficient signal-to-noise ratios. The above discussion partially explains the difference in signal-to-noise ratio in the spectra of different ions (Fig. 1). In Si IV, we obtain about 3 times the S/N of York et al. (1983). To the extent feasible, the dates of the new observations were based on monitoring of low-resolution spectra obtained periodically, to assure maximum flux for the program. The

TABLE 2
3C 273 FLUX

Line	Continuum Flux ^a (ergs cm ⁻² s ⁻¹ Å ⁻¹ [10 ⁻¹³])	Normalized Flux
Si IV 1393	6.6	1
Si IV 1402	3.0	0.45
Si II 1526	1.7	0.26
C IV 1548, 1550	1.7	0.26
C II 1334	2.0	0.30
H I 1215	2.6	0.39
Al III 1854, 1862	1.4	0.21
Fe II 1608	1.7	0.26

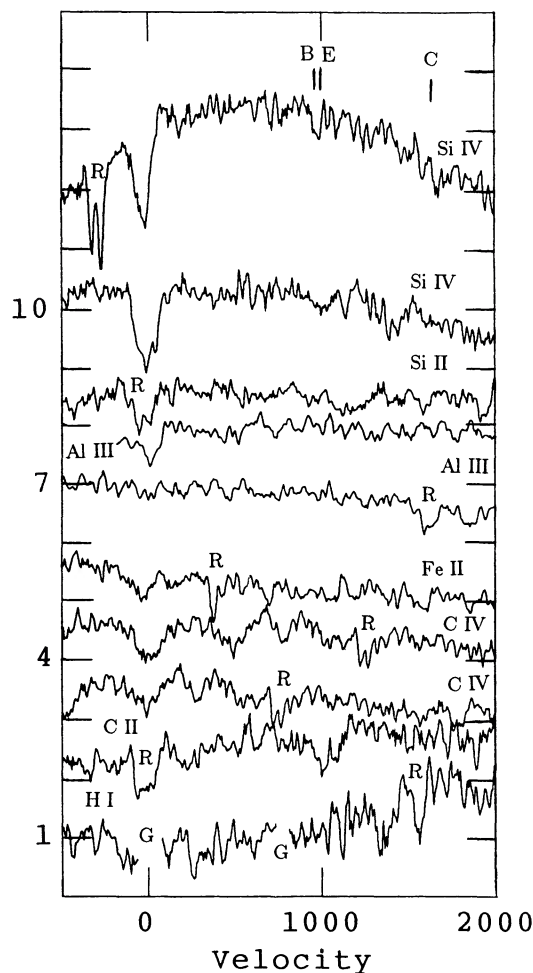
^a From Kinney et al. 1990, Fig. 20a.

FIG. 1.—Extracted data for 3C 273. The 10 spectra are shown in velocity space of the lines listed from ~ 500 to 2000 km s^{-1} . The spectra are shown in relative units. The bottom has a zero point at 1. Each spectrum is offset one unit above the previous one. Numbered tick marks on the ordinate correspond to the zero levels for the respective spectra. Reseau marks are shown by the letter R. The average velocity of the Virgo Cluster ellipticals is denoted by E and the average velocities of the B and C subgroups of the Virgo Cluster spiral galaxies are denoted by B and C. The position of the H I geocorona lines is denoted by G. The lines presented are, from top to bottom, Si IV 1402.770, Si IV 1393.755, Si II 1526.7066, Al III 1854.7164, Al III 1862.7895, Fe II 1608.4511, C IV 1548.195, C IV 1550.770, C II 1334.5323, and H I 1215.6737.

signal-to-noise ratios (S/N) of the ions studied are as follows: S/N $\sim 20/1$ for Si IV 1402; S/N $\sim 8/1$ for Si IV 1393 and Al III; S/N $\sim 5/1$ for Fe II and Si II; S/N $\sim 4/1$ for C IV; and S/N $\sim 3/1$ for C II. Leaving aside the Si IV lines, the noted variations in S/N arise from the wavelength-dependent spectral response of the *IUE* SEC Vidicon tube and the echelle spectrograph.

3. ANALYSIS

3.1. Profiles of Heavy Element Absorption Features

Figures 2 and 3 show the flattened and normalized spectra of the echelle orders containing spectral lines of common elements. Figure 2 shows, from top to bottom, Si IV 1393.755, Si IV 1402.770, C IV 1548.195, and C IV 1550.770. Figure 3 shows the Al III lines and the lines of singly ionized species, along with an H I profile of a point nearby in the sky, from the Bell Labs H I 21 cm survey (Stark et al. 1986). The 21 cm profile is offset to

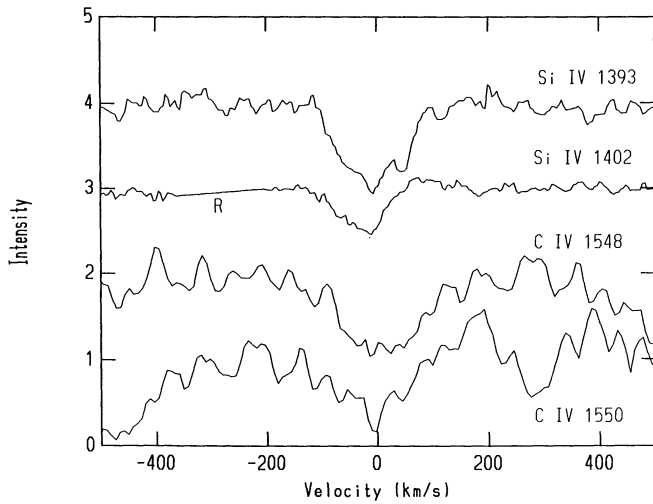


FIG. 2.—3C 273 Si IV and C IV. This figure shows flattened and normalized spectra of 3C 273 at the velocity of local interstellar absorption. They are, from top to bottom, Si IV 1393.755, Si IV 1402.770, C IV 1548.195, and C IV 1550.770. The reseau mark in the second line has been removed. The position of a reseau mark is denoted by R. The depression at 280 km s^{-1} in the C IV 1550 Å spectrum is unidentified and may be noise.

5.5 units and the profile shown is the antenna temperature $\times 2$. The other profiles are normalized to 1 and offset by 1 from the lower spectrum in each case. Reseau marks are denoted by R. The profiles shown are, from top to bottom, H I 21 cm, Al III 1854.7164, Al III 1862.7895, Fe II 1608.4511, Si II 1526.7066, and C II 1334.5323.

The C IV velocity width is noticeably greater than that of the other ions. In Figure 4 are shown the spectra of C IV 1548, Si IV 1393, and Si II 1526. The solid line is the spectrum of C IV. The crosses denote the Si II spectrum, and the circles denote the Si IV spectrum. The spectra are shown in velocity space and are normalized to 1. The C IV line is $\sim 20 \text{ km s}^{-1}$ wider in the positive velocities than are the Si IV and C II lines. This sight

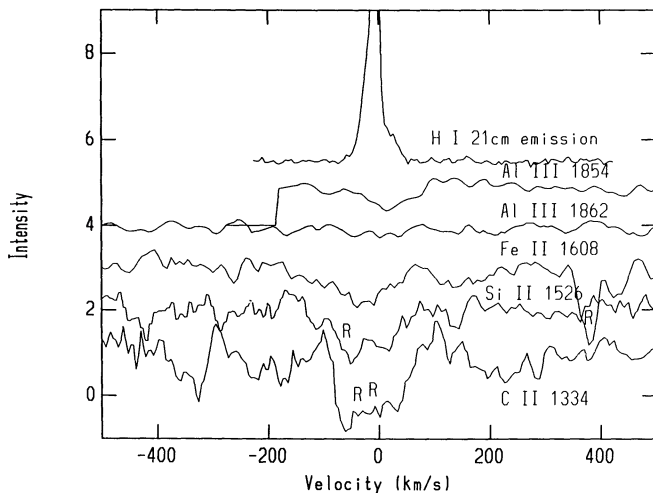


FIG. 3.—3C 273 H I and low ions. This figure shows flattened and normalized spectra of the Al III lines and the singly ionized lines, along with an H I profile. The 21 cm profile is offset by 5.5 units and the profile shown is the antenna temperature $\times 2$. The other profiles are normalized to 1 and offset by 1. Reseau marks are denoted by R. The profiles shown are, from top to bottom, H I 21 cm, Al III 1854.7164, Al III 1862.7895, Fe II 1608.4511, Si II 1526.7066, and C II 1334.5323.

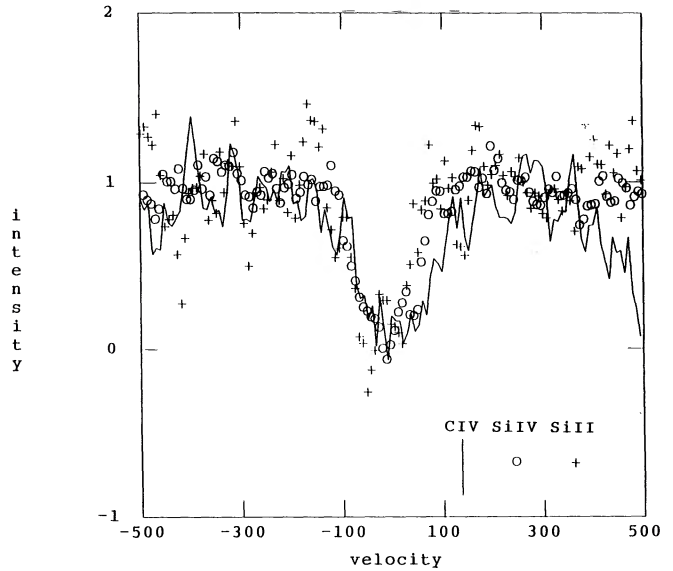


FIG. 4.—3C 273 C IV, Si IV, and Si II. The spectra of C IV 1548 is denoted by a solid line; Si IV 1393 is denoted by circles; and Si II 1526 is denoted by crosses. The spectra are shown in velocity space and are flattened and normalized to 1. The C IV profile is wider with excess absorption between 50 and 100 km s^{-1} .

line is similar to certain QSOs in which C IV is sometimes seen at velocities where Si IV is not seen. But, since there is only one C IV line with high enough signal-to-noise ratio to allow such a comparison, more observations should be made to allow for confirmation of this result.

3.2. Neutral Hydrogen

The Bell antenna has a beamwidth of 2° , and the symmetric beam is centered at $l = 290^\circ 22$, $b = 64^\circ 22$ about $0^\circ 3$ from 3C 273. The integral of the brightness temperature of the line gives a neutral hydrogen column density $N_{\text{HI}} = 1.8 \times 10^{20} \text{ cm}^{-2}$, for $T_{\text{spin}}(21 \text{ cm}) = 100 \text{ K}$. Cowie et al. (1981b) list three major H I components with $V_{\text{LSR}} = -17.6, -5.6, \text{ and } 20 \text{ km s}^{-1}$. The H I profile given here was modeled using Gaussians. The main components were modeled as being at $-18, -5, +6, \text{ and } +25 \text{ km s}^{-1}$, with weak emission at -57 km s^{-1} , and a possible very weak line at 158 km s^{-1} . The 158 km s^{-1} line has a peak antenna temperature of 0.06 K . Stark states that emissions of over 0.1 K are real and emission of over 0.05 K are probably real (Stark et al. 1986). The H I lines are almost certainly unresolved, due to the fact that the resolution of the Bells Labs survey is $\sim 5 \text{ km s}^{-1}$. Blades & Morton (1983) show Na I and Ca II components at ~ -20 and $+27$, as well as zero velocity gas.

The Lyman-alpha absorption line (Fig. 1, last frame) saturation extends to a velocity of about $+700 \text{ km s}^{-1}$. Absorption reaches the continuum near 1600 km s^{-1} , though the exact velocity is difficult to determine due to the reseau mark near 1600 km s^{-1} . The half-width half-maximum (HWHM), assuming a symmetric Voigt profile for the H I Galactic absorption, for $N_{\text{HI}} = 10^{20} \text{ cm}^{-2}$, is $\sim 2.5 \text{ \AA}$. The width of such a line increases as $(N)^{1/2}$. The half-width half-maximum is $1100 \pm 150 \text{ km s}^{-1}$, or 4.5 \AA , corresponding to $N(\text{H I}) \sim 3.2 \pm 1.1 \times 10^{20} \text{ cm}^{-2}$. This value is larger than the value obtained from 21 cm emission. A better continuum and better data on both sides of the line are required to get a more exact value. Perhaps the spin temperature of the H I is larger than

the 100 K assumed to interpret 21 cm emission-line data or there is hydrogen at velocities $< 1000 \text{ km s}^{-1}$ blended with the main H I near zero km s^{-1} , but unresolved so the absorption argument based on width leads to an upper limit.

The main point is to notice that an equivalent to the Galactic column density cannot exist at the 1000 km s^{-1} Virgo velocity, given the positive signal 2 \AA away ($+1500 \text{ km s}^{-1}$ in Fig. 1). There is no evidence for $N(\text{H I})$ at 1000 km s^{-1} being above 10^{15} cm^{-2} , though we cannot exclude systematic errors in our poor H I spectrum. The strict upper limit from Ly α is $N(\text{H I}) < 7 \times 10^{19} \text{ cm}^{-2}$, at the 1000 km s^{-1} Virgo velocity, since that column density would yield wings still rising where the observed spectrum flattens out.

3.3. Line Strengths and Velocity Widths

Equivalent widths, inferred column densities, and full width at half-maximum absorption measurements are given in Table 3. The first column contains the line wavelength; the second, the equivalent width of the absorption feature and formal error; the third, column density; the fourth, the velocity range of half-maximum absorption; the fifth, the half-maximum absorption width in km s^{-1} ; and the sixth, whether the line was modeled over the entire range of absorption, or the positive velocities. Formal errors in equivalent widths are 2σ , defined by the equation

$$\Delta W(2 \sigma) = 2 \times \Delta I \times \Delta \lambda \times (N)^{1/2},$$

where ΔI is the root mean square of the residuals, over a typical stretch of the continuum between the normalized spectrum and 1; $\Delta \lambda$ is the wavelength separation of points in the spectrum; and N is the number of points in the absorption line. Other possible errors come from not properly setting the continuum or the background levels, either of which could give higher or lower equivalent widths than the actual ones. The extracted spectra do not go significantly below zero even on strong lines, such as C II, C IV, or Si IV. They only go below zero at the position of reseau marks. Thus, the uncertainty due to errors in background subtraction is expected to be slight, less than the errors defined above. Upper limits in the equivalent widths of C II and Si II are quoted instead of measured values because of the presence of reseau marks at or near the velocity

of those lines. In the case of Si II, the long-wavelength side of the line is far enough from the reseau marks so that the equivalent width at velocity greater than zero should be trustworthy. That value is listed separately.

The velocity widths given in Table 3 have an error of $\pm 10 \text{ km s}^{-1}$ due to the fact the spectra are lined up to the nearest pixel, and pixel-to-pixel difference comes out to about 10 km s^{-1} . The formal resolution of IUE is 25 km s^{-1} (Turnrose & Thompson 1984). Possible velocity structure may be detected in the Si IV 1393 \AA line. Wu et al. (1990) failed to detect C IV in low-resolution spectra ($W_\lambda < 300 \text{ m\AA}$), possibly because of a difficulty in determining the continuum value in the low-resolution spectrum. Blades et al. (1991), using a different technique for aligning the low-resolution spectra, give values of W_λ consistent with this paper.

The column densities given in Table 3 were derived from measurements of the diminution of light relative to the continuum, point by point, and determine the column density responsible for that diminution. This method is accurate when the line in question is resolved. The absorption lines noted here are not resolved in some cases. In such a case, the method tends to underestimate the contribution to the column densities from narrow saturated lines. So the column densities given should be considered lower limits in the case of strong lines.

There is a possible absorption feature in Fe II between 100 and 200 km s^{-1} . It could be associated with the possible 21 cm radio emission at $+158 \text{ km s}^{-1}$. The signal-to-noise ratio of this spectrum is low and a stronger statement is not possible at the time. The effect may just be noise. More data in the future would be useful. No other indication of high-velocity Galactic absorption is seen.

4. INTERPRETATION

4.1. Possible Galactic Absorption

4.1.1. Comparison with Other Absorption-Line Data

Studies of Magellanic Cloud and Galactic stars with $|z| > 1000 \text{ pc}$ have shown relatively strong ($> 200 \text{ m\AA}$) lines of C IV and Si IV, attributable to gas in our halo (Savage & de Boer 1981; Pettini & West 1982). In stars $|z| < 1000 \text{ pc}$, $W_\lambda >$

TABLE 3
3C 273 EQUIVALENT WIDTHS

Line	Equivalent Width (m \AA)	N^a (cm^{-2})	Half-Strength Velocity Range (km s^{-1})	FWHM (km s^{-1})	Velocity Range (km s^{-1})
C II 1334.532	< 545	...	$> -80, < 56$	< 136	All
C II* 1335.708	230 ± 110	$\geq 1.9 \times 10^{14}$	$-63, +30$	93	All
C IV 1548.195	742 ± 104	4.1×10^{14}	$-76, +73$	149	All
C IV 1550.774	567 ± 131	4.3×10^{14}	$-86, +65$	151	All
Al III 1854.720	461 ± 54	3.7×10^{13}	$-26, +70$	96	All
Al III 1862.795	160 ± 53	3.6×10^{13}	$-63, +48$	111	All
Si II 1526.708	< 590	...	$> -81, +34$	< 115	All
	177 ± 49	$\geq 8.0 \times 10^{13}$	0, 34	34	> 0
Si IV 1393.775	579 ± 38	1.5×10^{14}	$-76, +58$	134	All
	295 ± 30	6.5×10^{13}	0, 58	58	> 0
Si IV 1402.769	221 ± 27	6.1×10^{13}	$-75, +30$	105	All
Fe II 1608.451	564 ± 97	$\geq 7.1 \times 10^{14}$	$-76, +15$	91	All
H I 1215.670	10,000:	1.8×10^{20b}	$< -500, +750$	> 1250	> -500

^a Column densities derived assuming lines on the linear portion of the curve of growth. They are thus, minimal values for second ions. Uncertainties in N are percentagewise approximately the same as errors in equivalent widths for Al III, C IV, and Si IV, for the weakest lines are probably unsaturated.

^b From emission line, 21 cm, $N(\text{H I}) = 1.8 \times 10^{20}$. From Ly α , $N(\text{H I}) \sim 3 \times 10^{20} \text{ cm}^{-2}$.

50 mÅ are uncommon and only rarely seen (York et al. 1983; Cowie et al., 1981b, Savage & de Boer 1981). The C IV and Si IV equivalent widths measured in 3C 273 thus stand out as being quite strong compared to values from other locations in our Galaxy (Pettini & West 1982). The C IV equivalent width may increase further as one looks through the entire halo. If so, the strength of the lines in halo objects, where there are few OB stars, compared to the weaker line strength near OB stars, argues for a different ionization source in the outer halo (> 5 kpc) than in the disk.

The line of sight to 3C 273 is remarkable in that the line velocity widths of the highly ionized lines are wider than those of low ionization species. This result is not seen, for instance, in the Danly study of high-latitude, high- z stars (Danly 1987, 1989). Also, the combined C IV equivalent widths are larger than the widths of C II and C II*. This is uncommon in high-latitude stars in our galaxy (Wu et al. 1990, Table 3). By contrast, C IV equivalent widths comparable to C II equivalent widths are detected in several of the QSO absorption line systems studied (Wu et al. 1990; Kinney et al. 1991). This subject will be discussed in more detail in Burks (1992).

The spectra of SN 1987A give another view through the Galactic halo (Blades et al. 1988; Savage et al. 1989). SN 1987A has a longitude close to that of 3C 273, and a comparable but opposite latitude. Since both 3C 273 and SN 1987A provide high-latitude sight lines that penetrate most of the halo, the absorption lines in each spectrum should be similar if the far halo is responsible for the line strengths and if the supposed halo is moderately uniform. This is, however, not the case. The low-velocity line portions ($v < 100$ km s $^{-1}$) of the lines of the highly ionized species C IV and Si IV are at least 2 times stronger in the 3C 273 spectra than in the same lines in the SN 1987A spectra. The 3C 273 lines are symmetrical about zero velocity, while the high ions in the spectra of SN 1987A are at positive velocities only (Savage et al. 1989). Spectra of 3C 273 and SN 1987A showing Si IV interstellar absorption are presented in Figure 5. The SN 1987A profiles are from Frisch, Welty, & York (1992). The 3C 273 lines are closer in strength to the total W_λ of components at $v > 100$ km s $^{-1}$ in SN 1987A, attributed

to the LMC itself. Gas at the LMC velocity ($v > 100$ km s $^{-1}$) is presumably associated with the numerous O-B stars in the LMC, in particular in 30 Dor, whose stars provide the ionizing source (by radiation, shocks, or cosmic rays).

One reason for discrepant results toward 3C 273 and SN 1987A may be that 3C 273 lies near the edge of both radio loop I (which is associated with the North Polar Spur) and radio loop IV (Berkhuijsen 1971). The radio loops have been associated with supernovae events (Heiles 1982). The emission associated with the loop is seen in radio continuum (Berkhuijsen 1971), 21 cm (Cleary, Heiles, & Halsam, 1979; Heiles et al. 1980), and X-ray (McCammon et al. 1983; McCammon 1984). The X-ray flux is comparatively high near the 3C 273 in the 400 eV to 6 keV range as well as in the very bright 100–300 eV range. Thus shocked highly ionized gas is associated with Loop I; perhaps much of the excess in C IV absorption over that in the SN 1987A sight line, is due to Loop I.

4.1.2. Consequences of a Halo Interpretation

If one adopts the view that the Si IV and C IV absorption arises in an extended (and inhomogeneous?) halo, the consequences of the extragalactic radiation field can be explored. Donahue & Shull (1991) produced photoionization models of intergalactic clouds, which ignore radiative transfer. In their model, $N(\text{C IV}) > N(\text{C II})$ for $\log U > -2.9$, where $U = n_\gamma/n_{\text{H}}$ is the ratio of the density of ionizing photons to the total hydrogen density. At this level of U , photons heat the gas to temperatures greater than 12,000 K for metallicity ~ 0.3 if the photon source is the cosmic background from AGNs. The neutral hydrogen fraction then is $10^{-2.5}$. If the C IV line arises in one of the intermediate-velocity H I components toward 3C 273, which have $N_{\text{H}} = 10^{19}$ cm $^{-2}$, the ratio of $N(\text{H I})/N(\text{H I} + \text{H II})$ would lead to $N_{\text{HI}} = 10^{21.5}$ cm $^{-2}$. High-resolution (4 km s $^{-1}$) profiles for 3C 273 of the species S II, Zn II, C II, and C IV with *Hubble Space Telescope* should allow an excellent test of the predicted large column density of hydrogen and of the general idea that the UV background ionizes gas in halos (York 1982b; Sargent et al. 1979).

The Donahue & Shull model assumes an ionizing radiation flux of $J_0 \approx 10^{-21}$ ergs cm $^{-2}$ Hz $^{-1}$ for a QSO absorption system at $z = 2$. Bechtold et al. (1987) find that the QSO flux at $z = 0$ is approximately a factor of 50 lower than the flux at $z = 2$. The Bechtold et al. value, based on QSO systems is consistent with the values of ionizing radiation obtained by Songaila, Bryant, & Cowie (1989) and Reynolds (Reynolds 1987; Kutyrev & Reynolds 1989) from observations of H α emission from HVCs. In the model corrected for the use of extragalactic background flux at $z = 0$, $\log U > -2.9$ only if $n_{\text{H}} < 8 \times 10^{-5}$ cm $^{-3}$.

The column density of C IV is $N(\text{C IV}) \sim n_{\text{H}} l \times [N(\text{C})/N(\text{H})] \times [N(\text{C IV})/N(\text{C})]$, where n_{H} is the volume density of H atoms and l is the pathlength. Generally, $x \equiv N(\text{C IV})/N(\text{C}) < 0.2$ (Donahue & Shull 1990). If the gas has solar abundance, $N(\text{C IV}) = 3 \times 10^{21} n_{\text{H}} \times l$ (kpc), or l (kpc) = $0.08 N_{14}(\text{C IV})/x n_{-3}$, where N_{14} is in units of 10^{14} , and n_{-3} is in units of 10^{-3} . Thus, $l \sim 1.6$ kpc/ n_{-3} for the value of $N(\text{C IV})$ obtained in this work. This leads to a value of $l > 20$ kpc for ionization by a diffuse background that produces $N(\text{C IV})/N(\text{C II}) > 1$ ($n_{\text{H}} \sim 8 \times 10^{-5}$). Probably components in several separate velocity regions are needed to explain the total line widths. The Loop I radio boundary encloses 1–2 sr at a distance of 100–400 pc, so a diffuse gas of this volume is not consistent with the morphol-

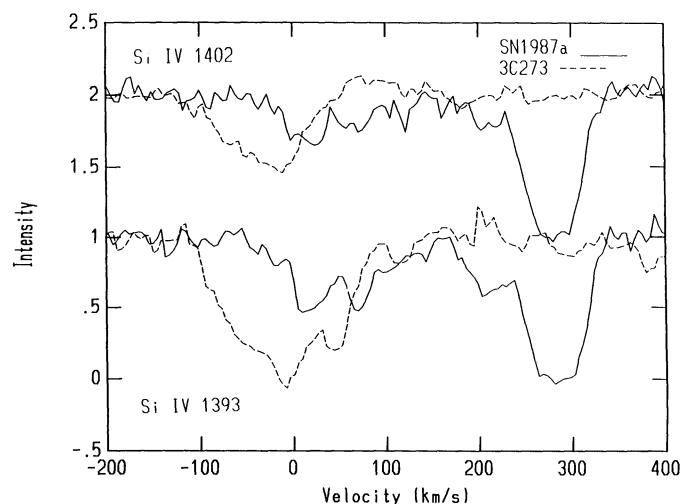


FIG. 5.—Si IV absorption. The spectra of 3C 273 and SN 1987A in the regions of Si IV interstellar absorption. The spectra are normalized and shown in velocity space. The Si IV 1393 spectra reach continuum levels at 1. The C IV 1402 spectra are offset by 1. The SN 1987A spectra are shown by solid lines. The 3C 273 spectra are shown by dashed lines.

ogy of the loop. However, a few dense shocks could generate adequate column densities.

Future observations may distinguish between the various possibilities noted above. If Loop I is responsible for the C iv absorption, regions in directions free of radio loops should show weak C iv. A uniform 5 kpc thick flattened halo (ionized by a source other than normal O–B stars or the extragalactic background) should show a latitude effect in C iv equivalent widths measured in random QSO sight lines. Clouds of low density and low pressure ($l > 5$ kpc) should show a patchy distribution of $W(\text{C iv})$ in a random set of QSOs, unrelated to disk structures such as Loop I.

4.1.3. Relationship of C iv and Other Indicators of the Halo Gas

Reynolds (1990) has reported diffuse Galactic H α emission over the entire sky. It arises from a low-density, 2–3 kpc, thick layer that has an emission-line spectrum significantly different from that of the traditional more localized H ii regions. He states that the very low intensity of [O III] and relatively strong [S II] indicate a low state of excitation with few ions present that require energies of greater than 25–35 eV for the ionization potential of the next lower ionization stage. And the presence of a substantial amount of warm H ii at high $|z|$ and along lines of sight far from ionizing stars seems to require either the existence of some as yet unidentified source of ionization or a special morphology of the H I in the Galactic disk that allows Lyman-continuum photons originating near the plane of the Galaxy to traverse the many parsecs from their source and reach the lower halo (Reynolds 1990). Sciama (1990) has proposed that neutrinos of mass 29 ± 1 eV could provide such an ionization source by decaying into ~ 15 eV photons.

The ionization potential from C I to C II is 11.3 eV, from C II to C III is 24.2 eV, and from C III to C IV is 47.9 eV (Allen 1973). Sciama's preferred hypothesis could lead to C II creation, but not C IV. The Reynolds observation concerning a dearth of highly ionized species forces the conclusion that the H α halo is not directly related to the region of domination of C iv.

The flux of diffuse soft X-ray (130–280 eV) near 3C 273, is one of the highest in the whole sky. This emission is associated with radio Loop I emission. Thus, it is plausible that C iv could be associated with EUV and soft X-ray flux from Loop I. The gas in this loop can also be collisionally ionized in shocks, thus creating C iv. The strong C iv absorption can be more easily explained by association with Loops I and IV, than by an ionization mechanism responsible for the more distant H α emission.

4.2. Absorption from the Virgo Cluster

The object 3C 273 is approximately 11° from the center of the Virgo Cluster. The 3C 273 coordinates are R.A. $12^{\text{h}}26^{\text{m}}33^{\text{s}}$, decl. $= +2^\circ19'42''$; the center of the Virgo Cluster is R.A. $12^{\text{h}}27^{\text{m}}$, decl. $+13^\circ30'$ (Mould, Aaronson, & Huchra 1980). Several galaxies in the cluster are less than 2° away from 3C 273 (de Vaucouleurs 1977). 3C 273 is less than 1° away from the large low-density gas cloud discovered by Giovanelli & Haynes (1989). The cloud is oriented at about the same position angle as the jet of 3C 273 (Arp & Burbidge 1990). $N(\text{H I}) > 10^{20} \text{ cm}^{-2}$ for some points in the $0^\circ.5$ cloud. The limit of detectability was about $6 \times 10^{18} \text{ cm}^{-2}$. A dwarf galaxy has been noted in this cloud (Djorgovski 1990). The cloud has an average velocity of 1275 km s^{-1} , while de Vaucouleurs (1982) found the average velocity of spirals and irregular galaxies in

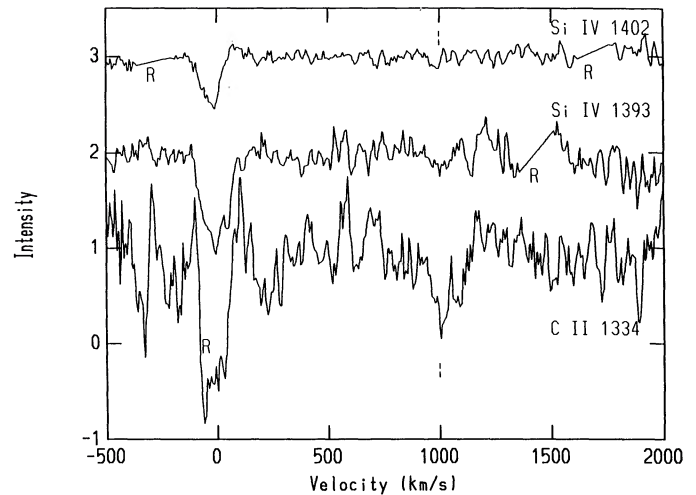


FIG. 6.—3C 273 Si iv and C II. The normalized C II and Si iv spectra from 3C 273 are shown in this figure, with a tick mark at 1000 km s^{-1} . Reseau marks are denoted by R. The lines are from, top to bottom, Si iv 1393.775, Si iv 1402.769, and C II 1334.532.

the cluster to be $\langle V_0 \rangle = 1165 \pm 133 \text{ km s}^{-1}$. De Vaucouleurs called the set of spirals and irregulars the S cloud. The E (ellipticals) cloud has a value of 1000 km s^{-1} . The above data have led to a revival of the proposal that 3C 273 is somehow associated with the Virgo Cluster (Arp & Burbidge 1990).

The spectra of 3C 273 were studied in order to find if there is absorption attributable to the Virgo Cluster. There was no obvious or consistent absorption detected at 1275 km s^{-1} or 1150 km s^{-1} . Possible absorption is seen in the Si iv 1393 Å, Si iv 1402 Å, and C II 1335 Å at a velocity of approximately 1000 km s^{-1} . The normalized C II and Si iv spectra are shown in Figure 6 with a tick mark at 1000 km s^{-1} . Reseau marks are denoted by R. Table 4 gives the equivalent widths and significance of detection that the measurements correspond to, in their respective spectra. To get a better velocity for the absorption, the three spectra were co-added with weighting for the total flux in each spectrum. The resulting spectrum is in Figure 7, which shows the region from ~ 500 to 2000 km s^{-1} . A local minimum of the spectrum is at 1000 km s^{-1} . C iv 1548 may have absorption at 1000 km s^{-1} , but reseau marks in this area cause difficulty in determining the correct continuum level, so the features in the C iv line may be attributable to noise. This line should be looked at in greater detail in the future.

Can this apparent absorption be attributed to the Virgo Cluster? The nearest small galaxy to 3C 273 seen in the Palomar sky survey plates has an angular size corresponding to 2 kpc on the print, and a minimum distance of 38 kpc from the line of sight of 3C 273, for a Hubble constant of $100 \text{ km s}^{-1} \text{ Mpc}^{-1}$, if the galaxy is at the Virgo distance. There are no spectral data for this galaxy. De Vaucouleurs (1982) divides the

TABLE 4
1000 km s^{-1} FEATURE

Ionic Line	Equivalent Width (mÅ)	σ
Si iv 1393	97	4.5
Si iv 1402	21	2.5
C II 1334	421	10.5

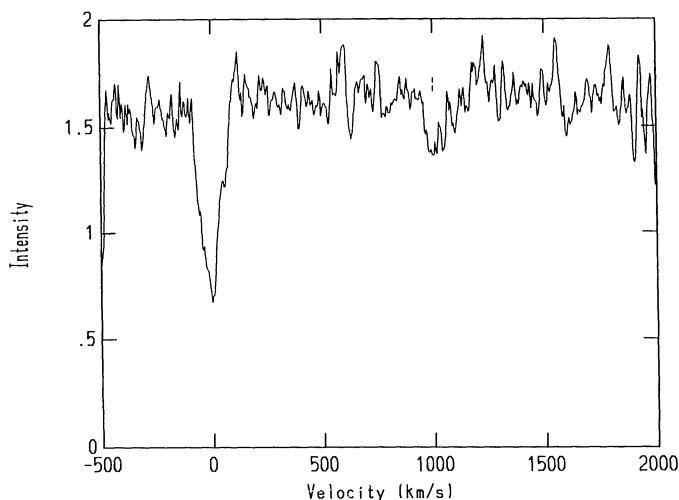


FIG. 7.—3C 2733 Si IV and C II composite. The weighted average of the spectra shown in Fig. 6. The spectrum is in velocity space, and the intensity is arbitrary. There is a tick mark at 1000 km s^{-1} .

Virgo S cloud (spirals and irregulars) into four groups which takes into account differences in kinematics and distance modulus. The four listed groups were A with $\langle V_0 \rangle = +77 \text{ km s}^{-1}$, B with $\langle V_0 \rangle = +975 \text{ km s}^{-1}$, C with $\langle V_0 \rangle = +1652 \text{ km s}^{-1}$ and D with $\langle V_0 \rangle = +2204 \text{ km s}^{-1}$. The velocities of specific galaxies have a large spread about these means. De Vaucouleurs' (1977) value for the average velocity of the Virgo E cloud (ellipticals and lenticulars) is $1000 \pm 60 \text{ km s}^{-1}$. A computed average for all galaxies within 6° of the center is $1029 \pm 53 \text{ km s}^{-1}$ (Mould et al. 1980). Thus absorption in C II and Si IV at 1000 km s^{-1} may be due to the Virgo Cluster.

Arp & Burbidge (1990) noted a possible association of the large H I cloud with the 3C 273 jet, as the cloud is aligned approximately with the jet. Arp and Burbidge studied this possible physical association and limited possible explanations for the connection to a heating of cold Virgo H I locally, by the jet. In this scenario 3C 273 was postulated to be in the Virgo Cluster, instead of at a cosmological distance. Since we are presumably looking down the directed jet, 3C 273 must be behind some H I. However, Figure 1 shows no obvious absorption which could be associated with the postulated material. Thus, the Arp and Burbidge hypothesis is not confirmed, though a detailed model would be required for a firm exclusion.

5. CONCLUSION

IUE was used to obtain high-dispersion spectra of the QSO 3C 273. The resulting spectra were studied in a search for interstellar absorption of various elements and ionizations. The spectra are probes of local gas, radio continuum Loops I and IV, the Galactic halo, and the Virgo Cluster. All Galactic absorption is contained within a velocity spread of approximately $\pm 110 \text{ km s}^{-1}$ in the lines of C II, C IV, Si II, Si IV, and Al III. No high-velocity absorption in these species is resolved

from absorption centered at zero. A region contiguous with 21 cm emission near $50\text{--}100 \text{ km s}^{-1}$ may contain only C IV.

Equivalent widths and absorption velocity widths of the high-ionization species are greater than those of low-ionization species. This result is unexpected compared with that observed from high- z , high-altitude halo stars. The Galactic absorption in the spectrum of 3C 273 is stronger than the presumed Galactic absorption in SN 1987A ($< 100 \text{ km s}^{-1}$), and comparable to the stronger absorption at the LMC velocity ($v > 100 \text{ km s}^{-1}$). The line of sight toward 3C 273 is more similar to that of QSO absorption-line systems than that usually found in a Galactic line of sight, where low-ionization species are stronger than high-ionization species. The increased C IV in the case of 3C 273 may be explained by an extended halo or by shocked gas associated with foreground radio loops. In the former case, the ionization source is unconnected with Galactic O-B stars. The extragalactic background could explain the result only for a photoionization model with $n_H < 8 \times 10^{-5} \text{ cm}^{-3}$. There may be a previously unidentified source of ionization by hot stars, or shocks of unidentified origin at large distances from the disk. Either suggestion (Loop I and/or IV, or extended halo gas) should be testable using absorption lines in spectra of Galactic objects in the direction of 3C 273, with distances between 0.1 and 10 kpc.

Possible absorption is seen at a velocity of 1000 km s^{-1} . This is near the average velocity of the elliptical galaxies in the Virgo Cluster and near the average velocity of the de Vaucouleurs B subgroup of spiral galaxies in the Virgo Cluster. Neither the nearby Giovanelli-Haynes cloud nor the Virgo C and D subgroups are detected in the data. Observations with *HST* would be desirable to try to confirm the possible absorption at 1000 km s^{-1} and to study the lines where *IUE* resseau marks have interfered with absorption-line measurements.

In January, a spectrum of 3C 273 was obtained with the Faint Object Spectrograph of the *Hubble Space Telescope*. Subsequent analysis has not confirmed the three features noted in Table 4 (Bahcall et al. 1991). However, H I Ly α absorption is seen at 1020 km s^{-1} and 1590 km s^{-1} . C II at the strength in Table 4 is ruled out, and Si IV 1393 Å at the strength in Table 4 is probably ruled out. The nature of the absorption near 1000 km s^{-1} bears further investigation.

The suggestion that the large Si IV value may be due to radio Loop I was made to one of us (D. G. Y.) after the strong Si IV lines toward 3C 273 became evident (York et al. 1983). The notion was rejected out of hand at the time but now appears reasonable. Unfortunately, the name of the individual who suggested it to us is not remembered.

R. B. and J. C. B. were supported by grant NAS5-875 for this work. G. B. and D. G. Y. were supported by NAG5-286 and NAG5-1715. Most of the observing was done from The University of Chicago campus, using a remote observing system paid for by a grant from the Block Board of the University of Chicago

REFERENCES

- Allen, C. W. 1973, *Astrophysical Quantities* (London: Athlone)
 Arp, H. C. & Burbidge, G. 1990, *ApJ*, 353, L1
 Bahcall, J. N., & Spitzer, L. 1969, *ApJ*, 156, L63
 Bahcall, J. N., Jannuzi, B. T., Schneider, D. P., Hartig, G. F., Bohlin, R. C., & Junkkarinen, V. 1991, *ApJ*, 377, L5
 Bechtold, J., Weymann, R. J., Lin, Z., & Malkan, M. A. 1987, *ApJ*, 315, 180
 Berkhuysen, E. M. 1971, *A&A*, 14, 260
 Blades, J. C., & Morton, D. C. 1983, *MNRAS*, 204, 317
 Blades, J. C., Wheatley, J. M., Panagia, N., Grewing, M., Pettini, M., & Wamsteker, W. 1988, *ApJ*, 334, 308
 Blades, J. C., York, D. G., Morton, D. C., & Wu, C.-C. 1991, in preparation
 Burks, G. S. 1992, in preparation
 Burks, G. S., York, D. G., Cowie, L. L., Songaila, A., Boksenberg, A., & Pettini, M. 1992, in preparation

- Cleary, M. N., Heiles, C., & Haslam, C. G. T. 1979, *A&AS*, 36, 95
- Cowie, L. L., Songaila, A., & York, D. G. 1981a, *ApJ*, 248, 956
- Cowie, L. L., Taylor, W., & York, D. G. 1981b, *ApJ*, 248, 528
- Danly, L. 1987, Ph.D. thesis, University of Wisconsin
- . 1989, *ApJ*, 342, 785
- de Vaucouleurs, G. 1977, *Nature*, 266, 126
- . 1982, *ApJ*, 253, 520
- Djorgovski, S. 1990, *AJ*, 99, 31
- Donahue, M., & Shull, J. M. 1991, *ApJ*, in press
- Frisch, P., Welty, D., & York, D. G. 1992, in preparation
- Giovanelli, R., & Haynes, M. P. 1989, *ApJ*, 346, L5
- Heiles, C. 1982, *ApJ*, 262, 135
- Heiles, C., Chu, Y., Reynolds, R. J., Yegingil, I., & Troland, T. H. 1980, *ApJ*, 242, 533
- Kinney, A. L., Bohlin, R. C., Blades, J. C., & York, D. G. 1991, *ApJS*, 75, 645
- Kutyrev, A. S., & Reynolds, R. K. 1989, *ApJ*, 344, L9
- McCammon, D. 1984, in *IAU Colloquium 81, Local Interstellar Medium*, ed. Y. Kondo, F. C. Bruhweiler, B. D. Savage (NASA CP-2345), 195
- McCammon, D., Burrows, D. N., Sanders, W. T., & Kraushaar, W. L. 1983, *ApJ*, 269, 107
- Morton, D. C. 1991, *ApJS*, 77, 119
- Mould, J., Aaronson, M., & Huchra, J. 1980, *ApJ*, 238, 458
- Pettini, M., & West, K. A. 1982, *ApJ*, 260, 561
- Reynolds, R. J. 1987, *ApJ*, 323, 553
- . 1990, in *IAU Symposium 139, The Galactic and Extragalactic Background Radiation*, ed. S. Bowyer & C. Leinert (Dordrecht: Kluwer), 157
- Sargent, W. L. W., Young, P. J., Bokserberg, A., Carswell, R. F., & Whelan, J. A. J. 1979, *ApJ*, 230, 49
- Savage, B. D. 1987, in *Interstellar Processes*, ed. D. J. Hollenbach & H. A. Thronson (Dordrecht: Reidel), 123
- Savage, B. D., & de Boer, K. S. 1981, *ApJ*, 314, 561
- Savage, B. D., Jenkins, E. B., Joseph, C. L., & de Boer, K. S. 1989, *ApJ*, 345, 393
- Sciama, D. W. 1990, *Nature*, 348, 617
- Songaila, A., Bryant, W., & Cowie, L. L. 1989, *ApJ*, 345, L71
- Songaila, A., & York, D. G. 1980, *ApJ*, 242, 976
- Spitzer, L. 1978, *Physical Processes in the Interstellar Medium* (New York: Wiley & Sons)
- Stark, A. A., Bally, J., Linke, R. A., & Heiles, C. 1986, unpublished
- Turnrose, B. E., & Thompson, R. W. 1984, *International Ultraviolet Explorer Image Processing Manual Version 2.0 (Greenbelt: NASA)*
- Ulrich, M. H., et al. 1980, *MNRAS*, 192, 561
- Wu, C.-C., Caulet, A., York, D. G., Blades, J. C., Boggess, A., & Morton, D. C. 1990, *ApJ*, submitted
- York, D. G. 1982a, *ARA&A*, 20, 221
- . 1982b, in *Advances in Ultraviolet Astronomy: Four Years of IUE Research*, ed. Y. Kondo & J. M. Mead (Greenbelt: NASA) 123
- York, D. G., Blades, J. C., Cowie, L. L., Morton, D. C., Songaila, A., & Wu, C.-C. 1982, *ApJ*, 255, 467
- York, D. G., Wu, C.-C., Ratcliff, S., Blades, J. C., Cowie, L. L., & Morton, D. C. 1983, *ApJ*, 274, 136